# Development of a Computational Model for Drug Release in the Nasal Cavity

A.H. Alexopoulos, P. Karakosta and C. Kiparissides

*Department of Chemical Engineering, Aristotle University of Thessaloniki*
*& Chemical Process Engineering Research Institute,*
*P.O. Box 472, 54124 Thessaloniki, Greece*

"New Frontiers", November 26-27, 2009



## Outline

- Introduction
  - ✓ A Roadmap to Nasal Vaccine Delivery Systems
  - ✓ Synthesis and In-vitro Studies of Nanocariers
- Computational Fluid Dynamics (CFD)
  - ✓ CFD Formulation
  - ✓ Cases Studied
- Particle Simulation
  - ✓ Particle Tracking in the Nasal Cavity
  - ✓ Particle Deposition
- Drug Release Model
  - ✓ Description and Model Predictions
- Conclusions

# Nasal Vaccination

- Vaccination is the most effective way of fighting infectious diseases like HIV, malaria, influenza, etc.
- Among the potential needle-free routes, nasal vaccination is particularly attractive.
- The nose is easily accessible (i.e., administration via drops or sprays) and the nasal cavity is equipped with a high density of dendritic cells (DC) that can mediate strong systemic and local immune responses against pathogens that invade the human body through the respiratory tract.

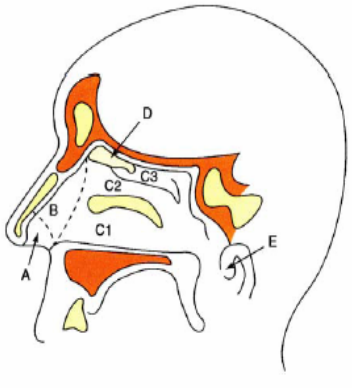


Sagittal section of human nasal cavity



# A Roadmap to Successful Nasal Vaccine Delivery

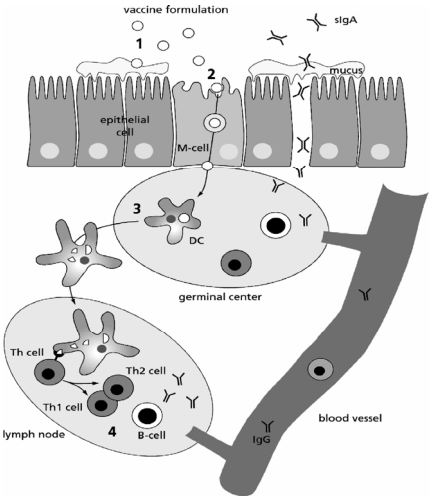


1. Prolonging the nasal residence time (mucoadhesion).
2. M-cell targeting (antigen uptake by M-cell transport).
3. Delivery to and subsequent activation/maturation of dendritic cells (DC).
4. Induction of cytotoxic T-lymphocyte immune responses.

Three major elements should constitute the nanostructure-based vaccines: the carrier, the antigen and the adjuvant (e.g., MPLA, CpG, etc.)

# Particle Synthesis

Synthesis of PLGA NPs by the Double Emulsion Method

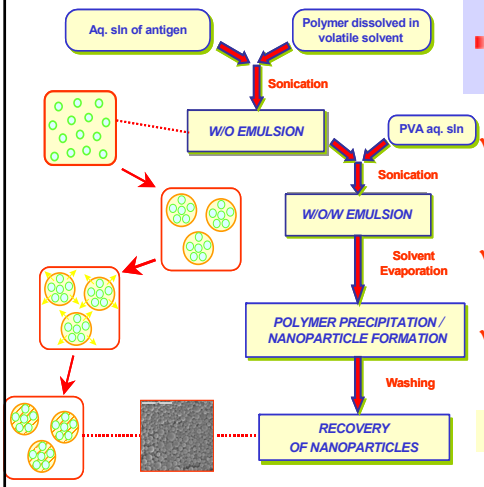


- PLGA: Resomer RG752H
- Antigen: Profos AG EndoGradeTM Ovalbumin, <1EU/mg
- Adjuvant: Monophosphoryl lipid A (MPLA)

✓ Various OVA and MPLA initial concentrations (0.15-10mg OVA, 200 μg – 2 mg MPLA)

✓ BSA-FITC loaded PLGA NPs for cell uptake studies

✓ OVA loaded and blank PLGA NPs as controls.

Synthesized amount per batch: ~ 60mg



# Characterization

- ✓ Surface morphology: SEM
- ✓ Particle size distribution: DLS
- ✓ Zeta potential: Aqueous electrophoresis measurements
- ✓ OVA & BSA-FITC loading: Bicinchoninic acid (BCA) protein assay
- ✓ MPLA loading: Limulus Amebocyte Lysate (LAL) kit
- ✓ WGA-FITC Quantification: UV (490nm)
- ✓ OVA integrity: Gel electrophoresis
- ✓ Cytotoxicity: MTS, LDH assays (*School of Biology, AUTh*)
- ✓ Endotoxicity: LAL & E-selectin induction (*JGU*)
- ✓ Haemocompatibility (*ULG*)
- ✓ Cell uptake: Confocal microscopy (*Institut Pasteur*)

# Surface Morphology & PSD

Blank PLGA NPs

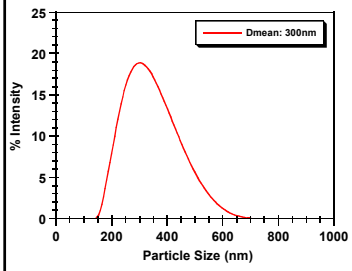


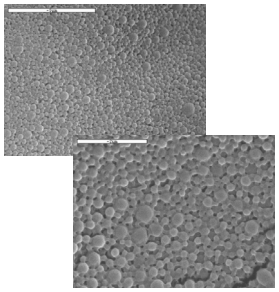

PLGA NPs Loaded with OVA & MPLA

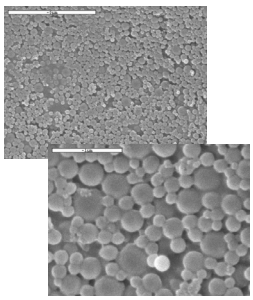

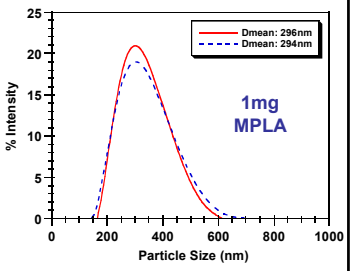


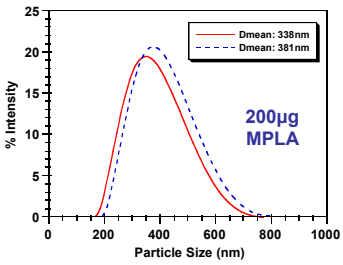


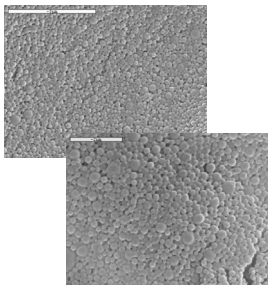



# PLGA NPs Loaded with OVA & **MPLA**

| Sample | Av. Diam. (nm) | Zeta potential (mV) | OVA loading (%wt) | MPLA loading (%wt) |
|---|---|---|---|---|
| DE-RG752H-OVA-MPLA-002 | 338 | -15.7 | 9.17 | 0.182 |
| DE-RG752H-OVA-MPLA-003 | 381 | -11.7 | 10.25 | 0.165 |
| DE-RG752H-OVA-MPLA-004 | 444 | -14.3 | 3.11 | 0.187 |
| DE-RG752H-OVA-MPLA-011 | 325 | -22.3 | 1.07 | 0.177 |
| DE-RG752H-OVA-MPLA-007 | 416 | -18.2 | 9.29 | 0.909 |
| DE-RG752H-OVA-MPLA-005 | 341 | -16.7 | 2.97 | 0.809 |
| DE-RG752H-OVA-MPLA-006 | 329 | -25.2 | 0.82 | 0.640 |
| DE-RG752H-OVA-MPLA-009 | 304 | -20.0 | 0.106 | 0.798 |
| DE-RG752H-OVA-MPLA-012b | 296 | -23.2 | 1.42 | 1.081 |
| DE-RG752H-OVA-MPLA-012c | 294 | -27.0 | 1.456 | 0.952 |
| DE-RG752H-OVA-MPLA-010 | 303 | -21.6 | 0.116 | 1.75 |

- ✓ OVA loading: 0.1 - 10 %wt
- ✓ MPLA loading: 0.16 - 1.75 %wt

# OVA Release Profile

Release profile of OVA from PLGA NPs in PBS at 37°C

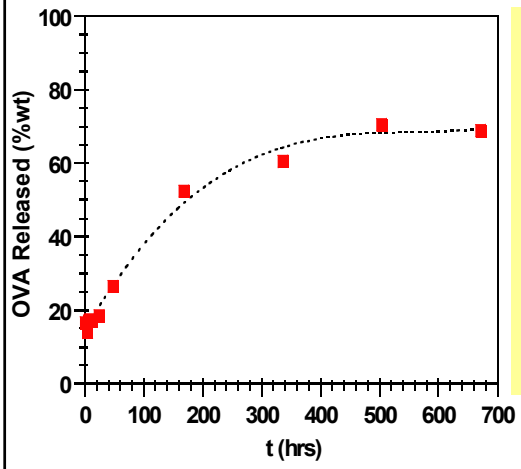


- Vials containing 1mg of NPs and 1ml of PBS were incubated at 37°C in a thermomixer at 1400rpm.
- At appropriate time intervals (2, 4, 8, 12, 24, 48, 1wk, 2,3,4wks) 1 ml sample of release medium was collected following centrifugation at 12,500rpm for 10min.
- The amount of OVA released from the NPs in the supernatant was measured by BCA.



# MPLA Release Profile

- The amount of MPLA released from the PLGA NPs in the supernatant was measured by LAL.

Release profile of MPLA from PLGA NPs in PBS at 37°C

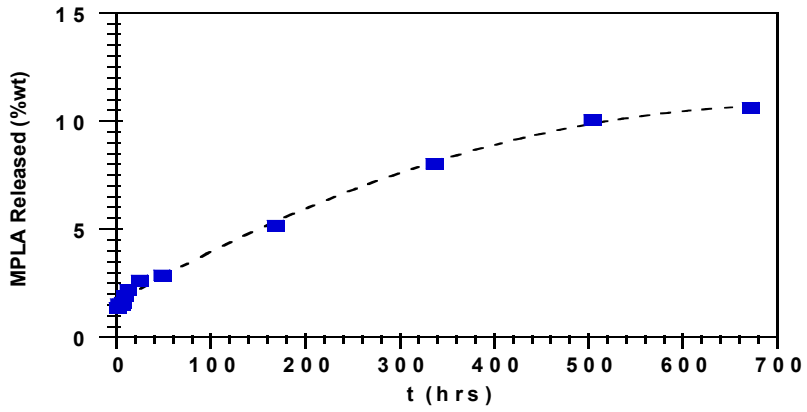

# Functionalization

- PLGA NPs containing OVA and MPLA (DE-RG752H-OVA-MPLA-005,6) were functionalized with wheat germ agglutinin - fluorescein isothiocyanate (WGA-FITC) by the carbodiimide method.

| Sample | Av. Diam. (nm) | Zeta potential (mV) | FITC-WGA (%wt) |
|---|---|---|---|
| DE-RG752H-OVA-MPLA-FWGA-006a | 356 | -22.8 | 0.146 |
| DE-RG752H-OVA-MPLA-FWGA-007a | 398 | -30.6 | 0.138 |
| DE-RG752H-OVA-MPLA-FWGA-0010a | - | - | 0.230 |

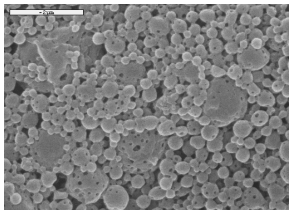

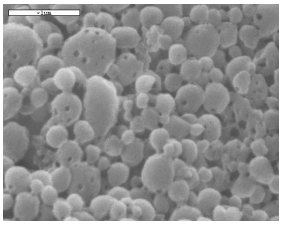



# Cell Uptake Studies

- Fluorescently labelled PLGA NPs were prepared for cell uptake studies.

| Sample | Av. Diam. (nm) | Zeta potential (mV) | BSA-FITC loading (%wt) |
|---|---|---|---|
| DE-PLGA-BSA-FITC-001 | 297 | -11.8 | 4.58 |
| DE-PLGA-BSA-FITC-002 | 302 | -10.53 | 5.10 |
| DE-PLGA-BSA-FITC-003 | 289 | -9.91 | 5.64 |

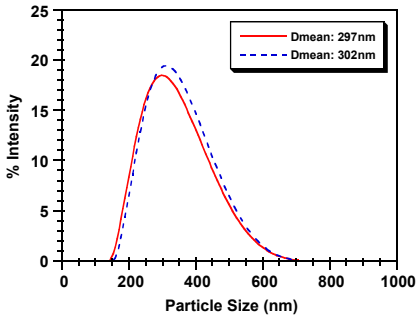


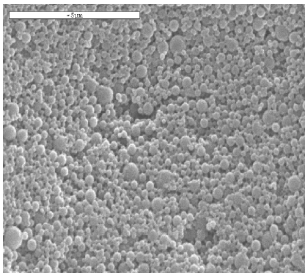

✓ The NPs were reported to be non-cytotoxic (MTS & LDH release assays).

# Cell Uptake

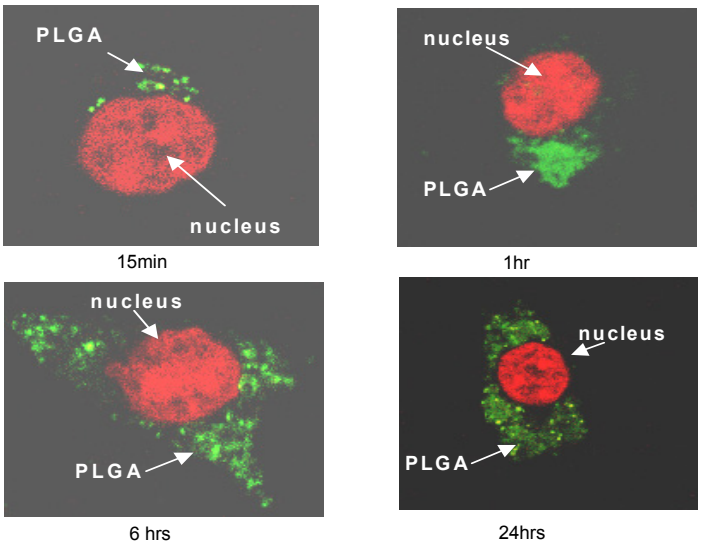


Cell uptake of BSA-FITC loaded PLGA NPs (cell line J774)



# Drug Delivery in the Respiratory Tract

- A virtual physiological model of the respiratory system is being developed, including the nasal cavity, the pharyngotrachea, and the pulmonary tract (bronchi, bronchioli, and alveoli).
- CFD simulations of each respiratory compartment are performed and connected together through the inlet and outlet boundary conditions.
- Drug delivery models are developed providing the amount of drug released from deposited particles and droplets.

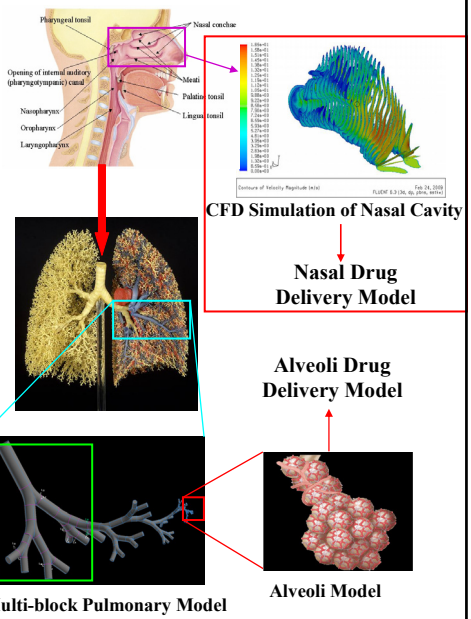

# Geometry of Nasal Cavity

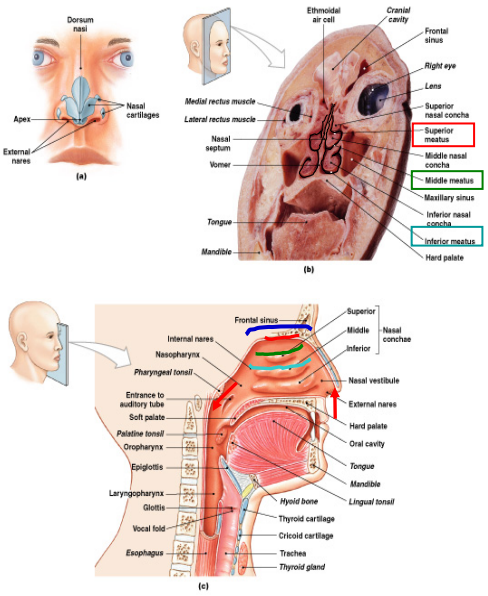


Nasal cavity geometry and symmetry differs significantly between people (more so than other physiological structures of the pulmonary system). **Length of Nasal Cavity**:10-11cm: **Airflow**: 15-25 l/min

**Mucosal transport velocity**: 5mm/min

Air flows into the nasal cavity through the nostrils undergoing a 70-90° turn into the nasal valve region. Three nasal conchae separate the nasal cavity into three regions, namely, superior, middle and inferior meatus.

The olfactory region is situated above the superior turbinate.

The structures converge again to the nasopharynx at the end of the nasal cavity from which airflow is directed to the outlet (pharynx).



# Geometry of Nasal Cavity

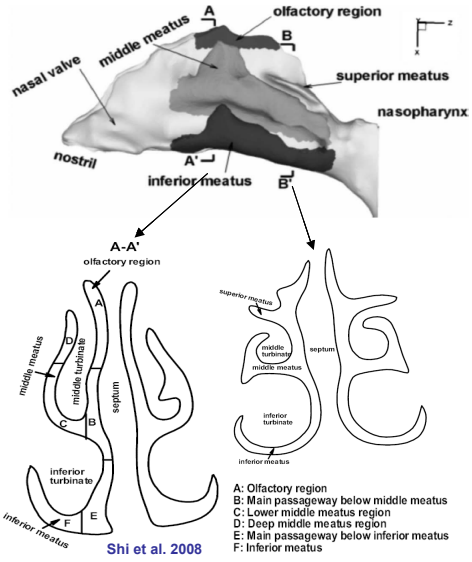


Air flows into the nasal cavity through the nostrils undergoing a 70-90° turn into the nasal valve region. Three nasal conchae separate the nasal cavity into three regions:

Superior, middle and inferior meatus regions

The olfactory region is situated above the superior turbinate.

The structures converge again to the nasopharynx at the end of the nasal cavity from which airflow is directed to the outlet (pharynx).

## Geometry of Nasal Cavity

- Construction of Nasal Cavity Geometry
  - ✓ Digital data (e.g., with CT or MRI)
  - ✓ In general 10-20 slices separated by 1 to 5mm are required to resolve the complex nasal cavity geometry
  - ✓ Geometry nasal cavity obtained from Shi et al. (2008)
- CAD/CAM
  - ✓ GAMBIT (FLUENT)
  - ✓ ICEM (FLUENT)
  - ✓ FIDAP (FED)
- Software
  - ✓ AMIRA
  - ✓ Flo Works

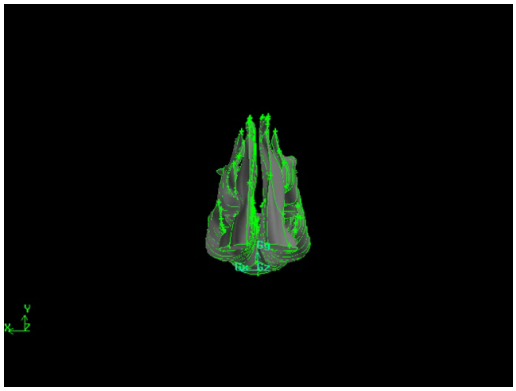



## Computational Fluid Dynamics

- Computational Fluid Dynamics (CFD) is a numerical approach that enables the study of the dynamics of flow as well as heat and mass transfer.
  - ✓ Equations of flow (Navier-Stokes), continuity, and heat-transfer are cast into a general system of equations for scalar quantities, φ:

$$\frac{\partial}{\partial t}\int_V \rho\phi dV + \int_A \rho\phi V dA = \int_A \Gamma\nabla\phi d\mathrm{A} + \int_V S\phi dV$$

- FLUENT 6.3 (software)
  - ✓ The equations for the scalar quantities, φ, are solved in each cell of grid.
  - ✓ The Finite-volume technique is used together with the Simplec method for pressure velocity coupling, and the Second Order Upwind method.
- Simulations performed:
  - ✓ The flow field calculations were conducted on a Dell 690 Workstation (eight-core Xeon 5300, 4Gb memory).
  - ✓ Simulations required 1-50hr per processor.

# Computational Grid

- Mesh Geometry was constructed in Gambit using Tetrahedra elements (i.e., as implement by TGrid in Gambit).

| Meshes | Type | Cells | Faces | Nodes |
|---|---|---|---|---|
| M1 | Basic | $1.24\ 10^6$ | $2.40\ 10^6$ | $0.26\ 10^6$ |
| M2 | Basic with outflow tube | $1.27\ 10^6$ | $2.63\ 10^6$ | $0.26\ 10^6$ |
| M3 | Basic with inflow tube | $1.32\ 10^6$ | $2.74\ 10^6$ | $0.27\ 10^6$ |
| M4 | Basic with refined surface region | $1.61\ 10^6$ | $3.51\ 10^6$ | $0.43\ 10^6$ |
| M5 | Polyhedra | $0.27\ 10^6$ | $1.76\ 10^6$ | $1.46\ 10^6$ |

- Different grids were constructed: with different types and numbers of cells (M1 and M5), with a cylindrical section attached to the inlet/outlet faces (M2 and M3), and with a refined surface region (M4).
- A cylindrical inlet tube was added (M3) to provide fully developed flow at the entrance of the nasal cavity.
- A cylindrical outlet tube was added (M2) to avoid recirculation at the outlet boundary conditions.



# CFD Results: Velocity Contours

- Simulations were performed for different inlet velocity magnitudes, profiles, and directions, different outlet conditions, different inlet turbulent intensities as well as different viscous models (e.g., laminar, k-ε, RNG k-ε, k-ω)

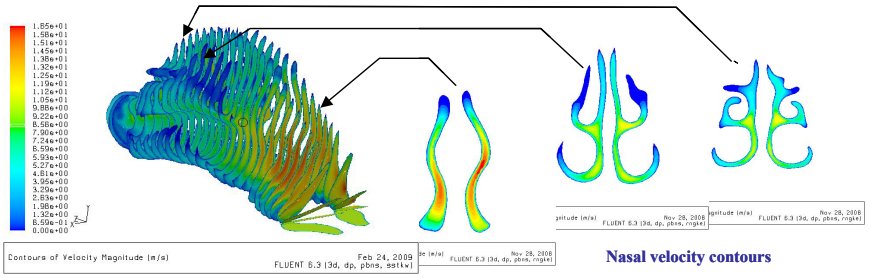


**Nasal velocity contours**

- The flow varies from laminar to turbulent. For inflow velocities $v_{in}$=1-2m/s (typical of regular breathing) we have Re=900-1800, respectively.
- The flow is strongly non-homogeneous. Largest velocity magnitudes occur in the region near the nasal valve. Flow is directed towards the regions where the nasal cavity meatuses intersect.
- Only limited flow reaches the outer tips of the meatuses and the olfactory region.

# CFD Results: Velocity Contours

- Effect of velocity magnitude

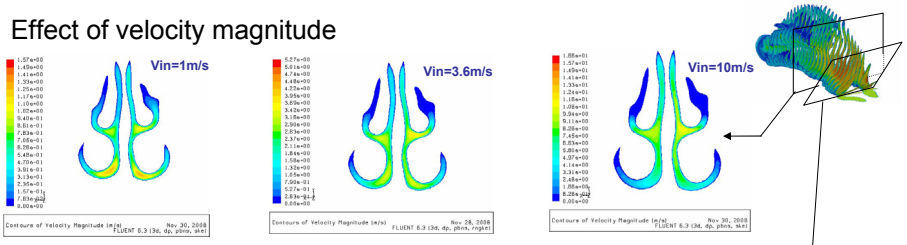


- Effect of inlet velocity angle (θ = is the angle between the direction of inlet and the direction of y-axis).

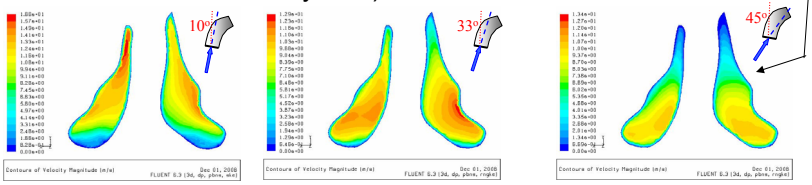


Large inlet velocity magnitudes direct the flow towards the middle meatus intersection. Inlet velocity angle affects the profiles only in the interior region of the nasal cavity.



# CFD Results: Contour Plots of Flow

- Sagittal plane contour plots of the x and y velocity components reveal the circulation patterns within the nasal cavity.

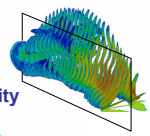

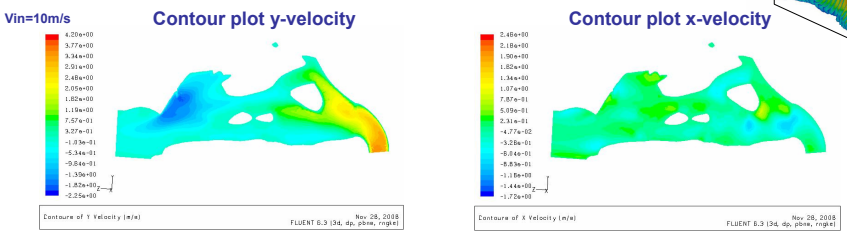


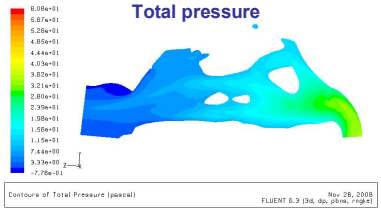


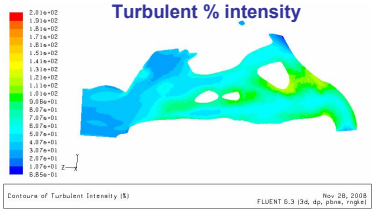

# Comparison with Shi et al. 2008

- Comparison based on coronal plane (i.e., x,y) velocity magnitudes and the axial dependence of the pressure and the Reynolds number.

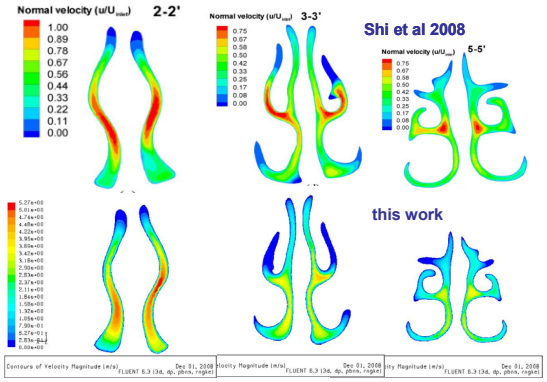


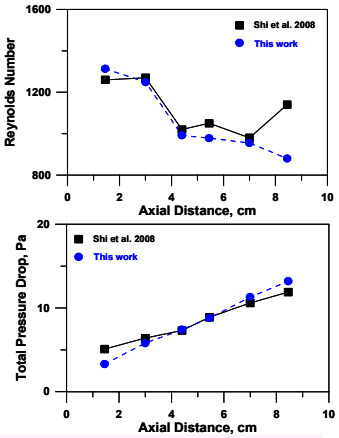


- The CFD simulations agree very well with the literature results of Shi et al. (2008) who employed a very similar geometry.



# Particle Simulations

## Equation of Particle Motion

$$\frac{du_p}{dt} = F_D\left(u - u_p\right) + \frac{g_x\left(\rho_\rho - \rho\right)}{\rho_\rho} + F_x$$

Drag force | Gravity force | Other forces (Brownian, Saffman, etc.)

where: $F_D = \frac{18\mu}{\rho_\rho d_\rho^{\,2}} \frac{C_D R_e}{24}$ and $C_D = \alpha_1 + \frac{a_2}{\mathrm{Re}} + \frac{a_3}{\mathrm{Re}^2}$ where: $\alpha_1$, $\alpha_2$, $\alpha_3$ are constants

- Particles of 1-20μm in size and inlet velocities between 1-10m/s the Strouhal number (Str=ωL/v) is 0.5-0.05 and the Womersley number (Wo=Rω/$\nu_{air}$) is 2-6 where ω is the inspiration frequency, L and R are the airway length and radius.
- The motion and deposition of particles 1 to 20μm in size is predominantly controlled by inertial forces.
- Particles are assumed to be released homogeneously from the inlet surface and are either constant in size or follow the Rosin-Rammler distribution.

$$f(D) = \exp\left(\frac{D}{D_0}\right)^n$$

where: $D_0$ is the mean diameter and n is the dispersion parameter

# Particle Streamlines

- Particle tracking was performed based on a CFD solution for fluid flow.
- Inertial forces dominate the deposition process of micron sized particles in the nasal cavity. Deposition of smaller (i.e., <1μm) particles is much smaller.
- Turbulent dispersion and surface roughness increased particles deposition.

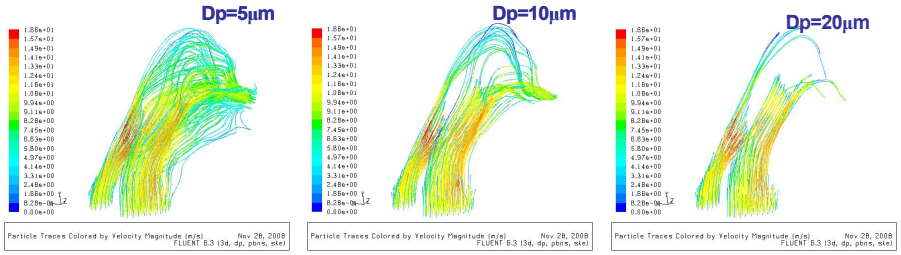


- Increasing particle size increases the total deposition fraction and also decreases the average axial deposition distance from the nostrils (i.e., $z_d$).



# Fractional Deposition In The Nasal Cavity

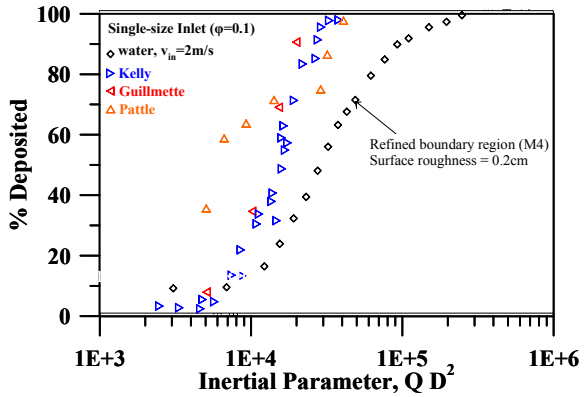


- Comparison of CFD results with experimental data (corresponding to different geometries).
- Results for different particle sizes, D, and inlet velocities, $v_{in}$, lie on in the same curve in terms of % deposition vs. impact factor, $QD^2$, where $Q = A\ v_{in}$.
- Both surface roughness and turbulent dispersion increased particle deposition.

# Particle Deposition Distribution

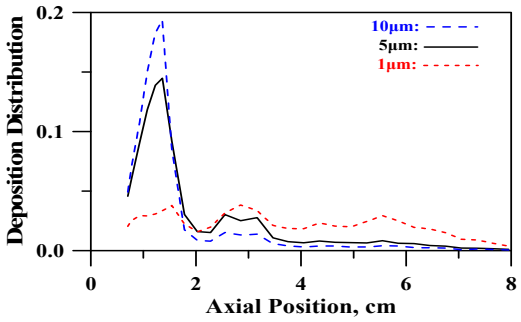


| Diameter, μm | Captured, % | Mean Axial Deposition, cm |
|---|---|---|
| 1 | 4.6 | ~5.5 |
| 2 | 7.1 | ~4.5 |
| 5 | 19.6 | 3.6 |
| 10 | 74.6 | 2.4 |
| 15 | 99.9 | 1.9 |
| 20 | 100 | 1.5 |

model k-ε, uniform diameter, $v_{in}$=10m/s

**Deposition distribution, $N_i$: Number of particles which deposit between $Z_i$ and $Z_{i+1}$.**

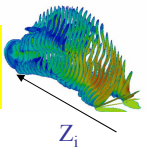


- The fractional particle deposition increased with particle size and inlet velocity.
- Average axial deposition length, $z_d$, decreased with particle size.
- Large particles (~10μm) deposit strongly in the anterior region of the nasal cavity.
- Small particles (~1μm) deposit more evenly throughout the length of the nasal cavity.

k-ω model , $V_{in}$=10m/s, zero turbulent dispersion and zero roughness
Rosin-Rammler distribution
Dispersion parameter =3.5, mean size = 1 and 10μm



# Bivariate Deposition Distribution

$D_{ave}$ = 1μm

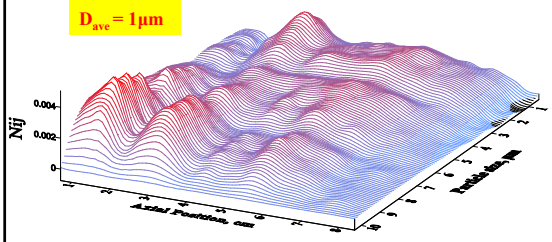


**Bivariate deposition distribution, $N_{ij}$: Number of particles in the size range $[D_j, D_{j+1}]$ which deposited between $Z_i$ and $Z_{i+1}$.**

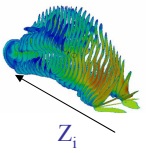


k-ω model
zero turbulent dispersion and zero roughness
Rosin-Rammler distribution,
$V_{in}$=10m/s inlet velocity
Rosin Rammler distribution
Dispersion parameter =3.5
Mean Size = 1 and 10μm
Mean Axial Deposition
10μm : 1.44cm
1μm : 3.23cm

$D_{ave}$ = 10μm

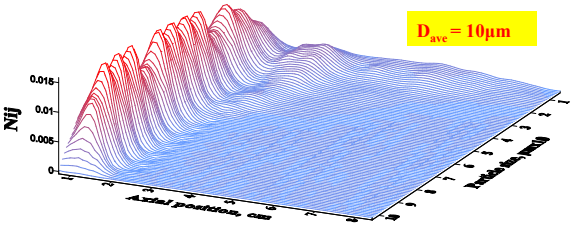


- Small particles (i.e., 1μm) deposit less than large particles (i.e., 10μm) but their deposition is much more uniform.

# Drug Release Model

- Experimental work by Pennington et al. (1988) and Harris et al. (1989) showed that the rate of drug release from droplet carriers increases with formulation viscosity.
- Deposited droplets have a finite residence time in the nasal cavity due to removal by motion of the nasal mucosa. The *residence time* $\tau$ depends on the deposition position according to:

$$\tau = \int_{z}^{L} 1/V_m(x)\,dx$$

- CFD simulations show that deposition position depends on the diameter according to:

$$z_d = 9.3 - 1.5\log(QD^2)$$

- Droplet diameters depend on the formulation properties. For example (Tanasawa & Toyoda 1955):

$$D = D_0\, N_G \left(\frac{\rho_L}{\rho_G}\right)^{0.25} \left[1 + 331\,\frac{We^{1/2}}{Re}\right]$$

where, $D_0$, is the nozzle diameter, We is the nozzle Weber number, Re is the nozzle Reynolds Number, and $N_G$, is given by:

$$N_G = \frac{\gamma\, g}{\rho_L}$$

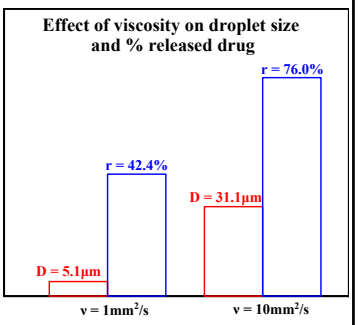


CFD simulations with k-ω model,
Vin=2m/s inlet velocity,
$D_0$=0.1cm, nozzle diameter
Single size droplet inflow

Increasing the formulation viscosity, **v↑**, increases the size of generated droplets, **D↑**, which decreases the mean axial deposition site, **z↓**, increasing the residence time, **τ↑**, resulting in a larger amount of released drug, **r↑**.



# Conclusions (1/2)

- ✓ PLGA NPs with average size ~300nm and relatively narrow PSD loaded with antigen & adjuvant as potential nanocarriers for nasal vaccination
- ✓ High encapsulation efficiency of OVA and MPLA independently of their initial concentrations
- ✓ Loading: 0.1-10%wt OVA, 0.16-1.75%wt MPLA
- ✓ Stable formulation for 4 weeks at 4°C
- ✓ Preservation of antigen integrity
- ✓ Release: ~70%wt OVA & ~11%wt MPLA released at 4wks
- ✓ Non-cytotoxic, endotoxin-free, haemocompatible formulation
- ✓ Uptake of PLGA nanocarriers by cells
- ✓ Functionalization of PLGA NPs with lectin for M cell targeting (proof of concept with WGA-FITC)

## Conclusions (2/2)

- ✓ Airflow through the nasal cavity is directed through the regions of largest cross-sectional area such as the meatus intersections.
- ✓ After the nasal valve the air velocity magnitude decreases and recirculation patterns appear distributing flow along the meatuses and up to the olfactory region.
- ✓ The deposition of particles in the size range of 1-20 μm for inhalation rates between 1-20 m/s is controlled by inertial forces. The deposition efficiency is a function of the impact factor, $QD^2$.
- ✓ Although small particles (~1μm) deposit less than large particles (~10μm) they are distributed much more evenly throughout the nasal cavity.
- ✓ A simple drug release model has been developed based on CFD simulations and droplet deposition distribution. The model predicts an increase in the amount of drug released from deposited droplets with an increase in droplet viscosity.



*CPERI/AUT* *Laboratory of Polymer Reaction Engineering*

# Formulation for Nasal Vaccination

- Dispersion of PLGA NPs containing antigen & adjuvant in 9%wt aqueous sucrose solution
- Sterilization in a UV incubator for 20 min

| Well # | NPs gel |
|---|---|
| 1 | MW |
| 2 | OVA |
| 3 | w/o UV |
| 4 | w UV |

- ✓ The formulation was reported to be sterile after being checked by i) plate assay and ii) incubation in rich medium without antibiotics *(JGU)*
- ✓ OVA integrity was found intact following UV sterilization

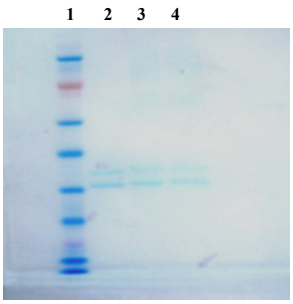


OVA integrity following UV sterilization



# MPLA Loading

- A Limulus Amebocyte Lysate (LAL) kit was used for the quantification of MPLA.
- MPLA solutions in water at concentrations of 0.001 – 10 ng/ml were assayed with LAL using a microplate reader (BioTek EL808IU-PC) for establishing a calibration curve.
- MPLA was quantified in the supernatants.

LAL is a quantitative kinetic assay for the detection of Gram-negative bacterial endotoxin.

It utilizes the initial part of the LAL endotoxin reaction to activate an enzyme, which in turn releases p-nitroaniline from a synthetic substrate, producing a yellow color.

The time required before color appearance (Reaction Time) is inversely proportional to the amount of endotoxin present.

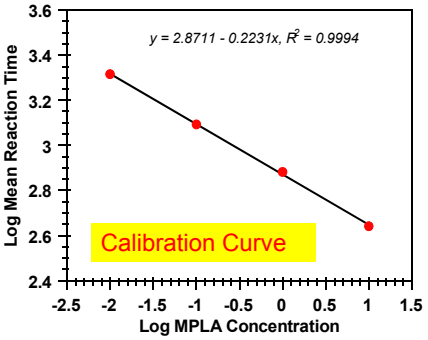

# Stability

Stability of PLGA NPs Loaded with OVA & MPLA in 9%wt Sucrose Solution

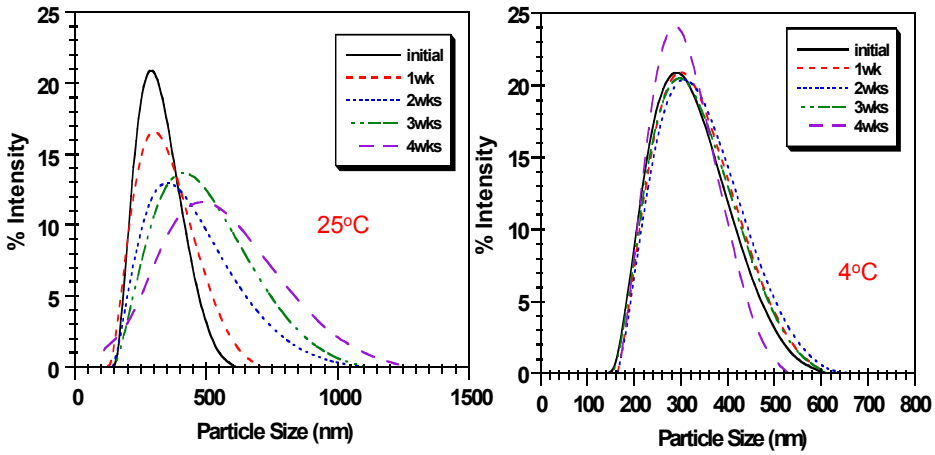




# OVA Integrity

- OVA loaded PLGA NPs were dissolved in 0.1N NaOH.
- Blank PLGA NPs were also dissolved in 0.1N NaOH.
- All samples (blank, 1wk, 2wk, 3 wk and 4wk) were centrifuged and gel electrophoresis was performed on the supernatants.
- For OVA gel electrophoresis, an aqueous solution of OVA was used.

Gel Electrophoresis of OVA loaded PLGA NPs incubated in PBS

| Well # | NPs gel |
|---|---|
| 1 | MW |
| 2 | OVA |
| 3 | blank NPs |
| 4 | 1wk NPs |
| 5 | 2wk NPs |
| 6 | 3wk NPs |
| 7 | 4wk NPs |

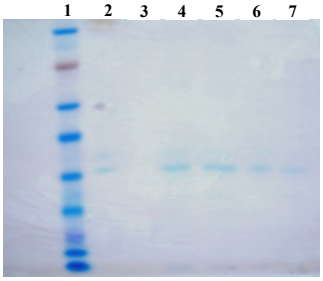

# In vitro Toxicity Studies

- OVA loaded PLGA NPs were examined with respect to their cytotoxicity, endotoxicity and haemocompatibility.

| Sample | Av. Diam. (nm) | Zeta potential (mV) | OVA loading (%wt) |
|---|---|---|---|
| DE-RG752H-OVA-004 | 319 | -19.5 | 0.255 |

- ✓ The Caco-2 cells viability was found to reduce for concentrations greater than 400 μg/ml (MTS assay).
- ✓ The NPs cytotoxicity does not change by increasing their concentration up to 500 μg/ml (LDH release assay).
- ✓ The NPs were reported to be endotoxin-free (LAL & E-selectin induction)
- ✓ No significant alteration of the haematological parameters was observed due to the NPs.



# In vitro Cytotoxicity